

Research Article

Synthesis and Characterization of Low Loss Dielectric Ceramics Prepared from Composite of Titanate Nanosheets with Barium Ions

Aleksandra Wypych-Puszkarz,¹ Izabela Bobowska,¹
Angelika Wrzesinska,¹ Agnieszka Opasinska,¹ Waldemar Maniukiewicz,²
Piotr Wojciechowski,¹ and Jacek Ulanski¹

¹Department of Molecular Physics, Faculty of Chemistry, Lodz University of Technology, Żeromskiego 116, 90-924 Lodz, Poland

²Institute of General and Ecological Chemistry, Faculty of Chemistry, Lodz University of Technology, Żeromskiego 116, 90-924 Lodz, Poland

Correspondence should be addressed to Aleksandra Wypych-Puszkarz; aleksandra.wypych@p.lodz.pl

Received 28 February 2017; Revised 23 April 2017; Accepted 14 May 2017; Published 14 June 2017

Academic Editor: Claude Estournès

Copyright © 2017 Aleksandra Wypych-Puszkarz et al. This is an open access article distributed under the Creative Commons Attribution License, which permits unrestricted use, distribution, and reproduction in any medium, provided the original work is properly cited.

We report a strategy for preparing barium titanate precursor, being the composite of titanate nanosheets (TN) with barium ions (Ba-TN), which subjected to step sintering allows obtaining TiO₂ rich barium titanate ceramics of stoichiometry BaTi₄O₉ or Ba₂Ti₉O₂₀. These compounds are important in modern electronics due to their required dielectric properties and grains' size that can be preserved in nanometric range. The morphology studies, structural characterization, and dielectric investigations were performed simultaneously in each step of Ba-TN calcinations in order to properly characterize type of obtained ceramic, its grains' morphology, and dielectric properties. The Ba-TN precursor can be sintered at given temperatures, so that its dielectric permittivity can be tuned between 25 and 42 with controlled temperature coefficients that change from negative 32 ppm/°C for Ba-TN sintered at 900°C up to positive 37 ppm/°C after calcination at 1300°C. XRD analysis and Raman investigations performed for the Ba-TN in the temperature range of 900 ÷ 1250°C showed that below 1100°C we obtained as a main phase BaTi₄O₉, whereas the higher calcinations temperature transformed Ba-TN into Ba₂Ti₉O₂₀. Taking into account trend of device miniaturization and nanoscopic size requirements, temperatures of 900°C and 1100°C seem to be an optimal condition for Ba-TN precursor calcinations that guarantee the satisfactory value of dielectric permittivity ($\epsilon = 26$ and 32) and ceramic grains with a mean size of ~180 nm and ~550 nm, respectively.

1. Introduction

Barium titanate ceramic materials have long history in electrotechnical applications. These dielectric oxide ceramics serve as microwave resonators and they are main components of many devices like cellular phones, global positioning system, and environmental monitoring systems on satellites [1]. The main aim of research in this area is to develop new materials or improve properties of already known systems (i.e., reducing dielectric loss and increasing dielectric permittivity). Recent revolutionary changes in wireless communication were achieved by reducing size and cost of components

made from improved microwave ceramics. Wide variety of polytitanates has been synthesized and characterized up to now. Among them, particularly a BaO-TiO₂ system with Ti rich region is interesting because it exhibits eligible electrical properties like good electrical permittivity and low dielectric loss at radio frequencies. BaTi₄O₉, BaTi₅O₁₁, and Ba₂Ti₉O₂₀ are prominent low loss dielectric compounds in this group. BaTi₄O₉ as dielectric ceramic was for the first time reported by Masse et al. [2] at early 1970 and had a huge contribution to a breakthrough in dielectric resonators ceramic technology. Conventional method for the preparation of BaTi₄O₉ is the solid state ceramic route by ball milling of

stoichiometric amounts of BaCO_3 and TiO_2 for about 24 hours [3, 4] and sintering at about 1100°C . It is then again ball milled, pelletized, and sintered at about 1350°C to achieve densification of the ceramic body. Wet chemical methods, such as oxalate [5] and citrate route [6] as well as modified Pechini method [7], were also applied for BaTi_4O_9 powders preparation. Cernea et al. [5] obtained BaTi_4O_9 from oxalates and documented its stable dielectric properties: dielectric permittivity $\epsilon = 38$, quality factor $Q = 3800 \div 4000$ at $6 \div 7$ GHz, and temperature coefficient $\tau_f = 11 \text{ ppm}/^\circ\text{C}$. Pure BaTi_4O_9 suffers from relatively high values of temperature coefficient, so it is not very suitable as dielectric resonator. Hence the dielectric properties of BaTi_4O_9 phase are often modified by using different additives [8]. $\text{BaTi}_5\text{O}_{11}$ synthesis was for the first time described by Tillmanns, but it was not pure phase but mixed with rutile [9]. Single-phase $\text{BaTi}_5\text{O}_{11}$ was prepared by wet chemical methods like citrate route [10] or sol-gel [11]. This phase is stable under heating up to 1200°C , then, it decomposes into TiO_2 , $\text{Ba}_2\text{Ti}_9\text{O}_{20}$, and/or BaTi_4O_9 . $\text{BaTi}_5\text{O}_{11}$ phase has higher dielectric constant and quality factor compared to BaTi_4O_9 ; however the values of τ_f are also higher. Fukui et al. prepared $\text{BaTi}_5\text{O}_{11}$ by sol-gel method after heating at 1120°C for 48 hours. Obtained samples exhibited dielectric permittivity equal to 42, $Q \times f > 60,000$ GHz, and $\tau_f = 39 \text{ ppm}/^\circ\text{C}$ [12]. $\text{Ba}_2\text{Ti}_9\text{O}_{20}$ can be conventionally synthesized by mixing BaCO_3 and TiO_2 in appropriate stoichiometry and calcined at about 1200°C , again milled, pelletized, and sintered at about 1400°C for 3 hours [13]. $\text{Ba}_2\text{Ti}_9\text{O}_{20}$ obtained by solid state synthesis usually coexists with BaTi_4O_9 phase as it is thermodynamically stable in the vicinity of the desired composition. However, pure phase synthesis was achieved by wet chemistry methods. Lu et al. [11] described synthesis based on mixing methanol solution of barium hydroxide with titania sol obtained from hydrolysis of titanium alkoxide. Obtained xerogel was stepwise heated up to 1100°C giving $\text{BaTi}_5\text{O}_{11}$ phase, while prolonged heating at 1200°C gave pure $\text{Ba}_2\text{Ti}_9\text{O}_{20}$. Fang et al. [14] prepared $\text{Ba}_2\text{Ti}_9\text{O}_{20}$ in reaction of BaTi_4O_9 with TiO_2 and sintering at 1390°C . Obtained sample showed grain size of about 2-3 micrometers and high sintered density of 99%. The dielectric permittivity was equal to 39, quality factor was 42000 GHz, and the temperature coefficient reached $5 \text{ ppm}/^\circ\text{C}$. BaTi_4O_9 and $\text{Ba}_2\text{Ti}_9\text{O}_{20}$ have similar values of dielectric permittivity and quality factors. BaTi_4O_9 has temperature coefficient close to zero and is always positive, while reported values of τ_f for $\text{Ba}_2\text{Ti}_9\text{O}_{20}$ are close to zero as well as being negative in some reports [10].

The method of mixing of two low loss ceramic materials with positive and negative temperature coefficient has become well known [15]. This kind of approach is very convenient for preparation of new materials with desired properties by simple selection of proper components. However, very often it is difficult to obtain material with expected intermediate properties because it is impossible to retain individual character of components during sintering process. Thus, development of new precursors of barium titanates and study of their temperature transformation and dielectric properties are still very attractive.

The aim of this work was to develop a method for TiO_2 rich barium titanates synthesis by employing titanate nanosheets (TN). They have an orthorhombic layered structure that is composed of corrugated host layers of edge-shared octahedra and interlayer (tetramethyl)ammonium ions (TMA^+) compensating for the negative charge which arises from substitution of lower valence metal ions or vacancies of Ti [16]. These TMA^+ ions are exchangeable with a variety of inorganic and organic ions and in this way the TN is an ideal candidate for host-guest chemistry as well as ion exchange [17]. The ion exchangeability also provided the opportunity to prepare precursor of ceramics. For example, potassium hexatitanate ($\text{K}_2\text{Ti}_6\text{O}_{13}$) was prepared by ion exchange, followed by heat treatment at 600°C [18]. Taking this into consideration, in this work we applied TN in ion exchange process to immobilize barium ions from solution. The obtained by this way composite, under a thermal treatment in moderate temperature in air, transformed to BaTi_4O_9 , $\text{BaTi}_5\text{O}_{11}$, and $\text{Ba}_2\text{Ti}_9\text{O}_{20}$ phases with desired dielectric properties.

2. Experimental Section

All reagents were used as received without further purification.

Synthesis. 250 ml aqueous solution of barium acetate monohydrate (5.45 g; 20 mol, purchased from Polish Chemical Reagents, POCH, Gliwice, Poland) was mixed with 250 ml aqueous colloidal solution of titanate nanosheets, TN (2.5 g; $R = 0,6$). The details of preparation and characterization of TN have been reported elsewhere [19]. After mixing solutions, ion exchange reaction between (tetramethyl)ammonium ions from TN and barium cations from barium acetate in aqueous environment led to precipitation of the powder. The mixture was heated for 10 h at room temperature under stirring and next without stirring for 10 h at 90°C . After the reaction, the precipitate was separated by centrifugation, washed with water until pH 7, and dried under vacuum. The total yield of dried organic-inorganic powder was 2.3 g and it is labeled as Ba-TN or precursor of barium titanate. The Ba-TN powder after reaction was subjected to calcination at 500°C for 1 hour and pressed to get a pellet under pressure of 436 MPa for 10 min. Based on thermogravimetric measurement (data not shown) temperature of 500°C was chosen as an optimal one that allows a decomposition of the organic part of the precursor and the evaporation of volatile products from the sample. The higher temperatures allow for thermal diffusion of the reagents throughout the volume to facilitate the reaction that produces barium titanate ceramic. The pellet was sintered at 900°C for 4 hours and then subsequently at 950°C , 1000°C , 1050°C , 1100°C , 1150°C , 1200°C , 1250°C , and 1300°C for 2 h in each temperature. The time of sintering was chosen according to research of Pfaff who found that at temperature higher than 900°C a densification parameter of BaTi_4O_9 is constant after two hours of heat treatment [20]. During the applied step sintering procedure the mean particle diameter was investigated and pellets' green density calculated simultaneously with its phase transformation and dielectric properties studies.

3. Characterization

Raman investigations were performed using a Fourier Transform Raman spectrometer (Bruker). All spectra were recorded in the macrochamber light scattering mode; the Raman spectra were obtained at 20°C using the Nd:YAG laser wavelength $\lambda = 1064$ nm.

Room temperature powder X-ray diffraction patterns were collected using a PANalytical X'Pert Pro MPD diffractometer in the Bragg–Brentano reflection geometry. Copper $\text{CuK}\alpha$ radiation was used from a sealed tube. Data were collected in the 2θ range 5–90° with a step of 0.0167° and an exposure per step of 20 s. The samples were spun during data collection to minimize preferred orientation effects. For phase analysis, the PANalytical High Score Plus software package was used combined with the International Centre for Diffraction Data's (JCPDS) powder diffraction file (PDF-2 ver. 2009) database of standard reference materials.

Particle sizes of Ba-TN obtained in different step of calcination were estimated from SEM images that were collected using a Hitachi S3400N scanning electron microscope with accelerating voltage of 25000 V.

The dielectric properties of synthesized sample were investigated using a Novocontrol GmbH Concept 40 broadband dielectric spectrometer equipped with Quatro Cryosystem in the frequency range of $10^{-1} \div 10^6$ Hz and in the temperature range of $-140^\circ\text{C} \div 200^\circ\text{C}$ (in steps of 10°C). The obtained complex dielectric function (ϵ^*) was measured by

$$\epsilon^* = \epsilon' - i\epsilon'' \quad (1)$$

where ϵ' and ϵ'' are the real and imaginary parts, respectively.

Before electric measurement each pellet was additionally dried at 90°C under reduced pressure in order to exclude the influence of the humidity. To provide good contact between the sample and external electrodes during electrical investigations, 150 nm thick gold electrodes were deposited on both sites of the pellet. The densities of the samples sintered at different temperatures were evaluated based on the external dimensions and mass of the pellets. The relative density of pellets was estimated through comparison with theoretical crystallographic density of the major crystallographic phase defined from Raman and XRD investigations.

4. Results and Discussion

Raman spectra of the samples before and after the ion exchange are shown in Figure 1. For TN in Figure 1(a), the spectrum is essentially the same as the data reported for titanate nanosheets intercalated by TMA^+ ions [21]. According to the literature [21, 22] Raman bands observed at 275 cm^{-1} , 384 cm^{-1} , 448 cm^{-1} , 662 cm^{-1} , 883 cm^{-1} , and 899 cm^{-1} can be attributed to the Ti-O lattice vibrations in the TiO_6 octahedral host layers and the strong peaks at 756 cm^{-1} and 954 cm^{-1} were related to (tetramethyl)ammonium ions (TMA^+). These two peaks just disappear after the exchange reaction-replacement (Figure 1(b)) of TMA^+ ions in TN by barium ions. The Raman vibration assigned to Ti-O still exists which is a convenient proof that 2D structure of TN

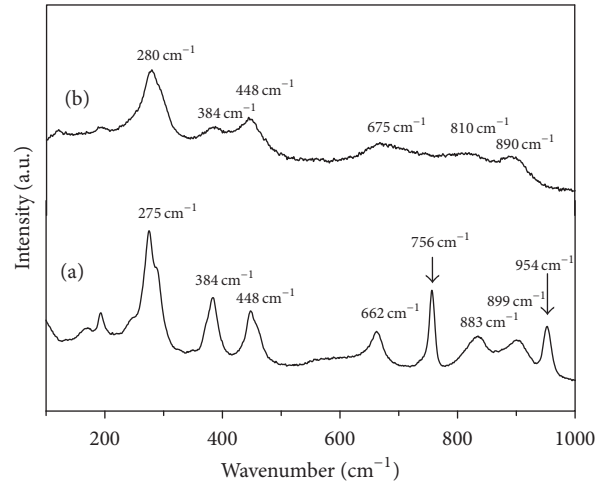


FIGURE 1: Raman spectra of dried (a) titanate nanosheets, TN, and (b) precipitate Ba-TN.

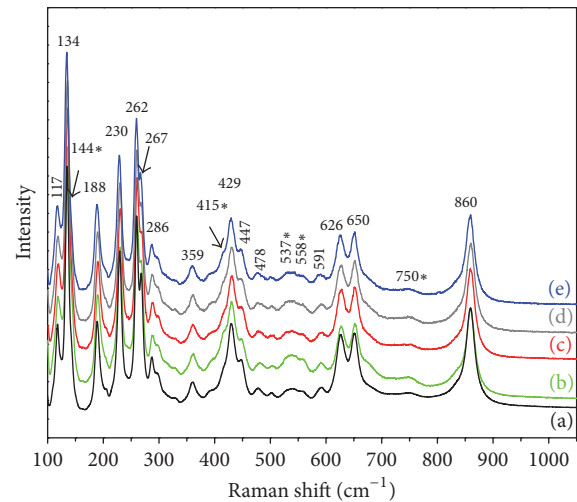


FIGURE 2: Raman spectra collected at room temperature for Ba-TN after sintering at (a) 900°C, (b) 950°C, (c) 1000°C, (d) 1050°C, and (e) 1100°C. Raman bands characteristic for $\text{BaTi}_5\text{O}_{11}$ are labeled by stars.

was preserved. However, peaks at $600\text{--}1000\text{ cm}^{-1}$ spectral region shift to lower frequencies which could be affected by a presence of Ba^{2+} ions in the interlayer of TN [23]. Obtained powder of Ba-TN could be considered as a precursor of BaTi_4O_9 since, after the thermal treatment at 900°C for 4 h, it gave the characteristic Raman spectrum for this compound (Figure 2(a)). One can observe bands located at 117 cm^{-1} , 134 cm^{-1} , 188 cm^{-1} , 230 cm^{-1} , 262 cm^{-1} , 267 cm^{-1} , 286 cm^{-1} , 359 cm^{-1} , 429 cm^{-1} , 447 cm^{-1} , 478 cm^{-1} , 591 cm^{-1} , 626 cm^{-1} , 650 cm^{-1} , and 860 cm^{-1} that are characteristic for BaTi_4O_9 [24] according to work of Rössel et al. Further sintering at temperature range between 950°C and 1100°C, during 2 h at each temperature, gave the Raman spectra of the same intensity and identical Raman bands as observed for Ba-TN sintered at 900°C (see Figure 2(b–e)). These results allow for conclusion that there was not any phase transformation

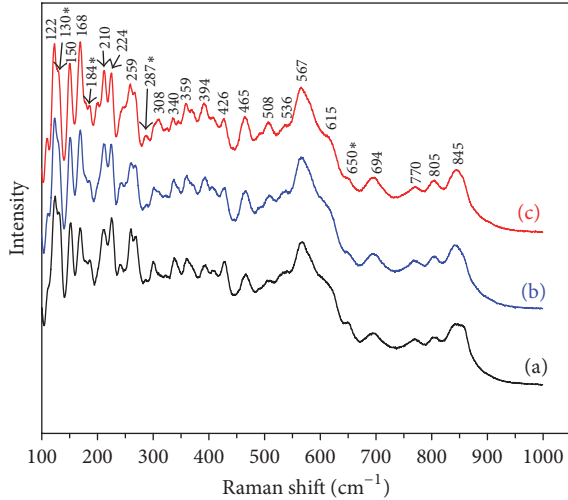


FIGURE 3: Raman spectra collected at room temperature for Ba-TN after sintering at (a) 1150°C, (b) 1200°C, and (c) 1250°C. Raman bands assigned to BaTi_4O_9 are marked by stars.

during the applied thermal treatment in the temperature range between 900°C and 1100°C. Moreover sharpness of Raman peaks denotes well crystallized structure that was independently revealed by X-ray diffraction studies. Detailed analysis of the recorded Raman spectra allowed observing bands of lower intensity which are located at 144 cm^{-1} , 415 cm^{-1} , 537 cm^{-1} , 558 cm^{-1} , and 750 cm^{-1} . They are marked by stars (in Figure 2) and their occurrence indicates the presence of barium titanate of stoichiometry $\text{BaTi}_5\text{O}_{11}$.

Figure 3 shows Raman spectra for Ba-TN precursor sintered for 2 h at (a) 1150°C, (b) 1200°C, and (c) 1250°C, on which one can observe a significant change of the spectra as compared to Raman spectrum of precursor sintered up to 1100°C. In Figure 3(a–c) there are Raman bands characteristic for BaTi_4O_9 phase that almost totally disappeared with exception of the bands located at 130 cm^{-1} , 184 cm^{-1} , 287 cm^{-1} , and 650 cm^{-1} . For the precursor sintered at the temperatures of 1150°C and higher, there are detected Raman bands located at 122 cm^{-1} , 150 cm^{-1} , 168 cm^{-1} , 210 cm^{-1} , 224 cm^{-1} , 259 cm^{-1} , 308 cm^{-1} , 340 cm^{-1} , 359 cm^{-1} , 394 cm^{-1} , 426 cm^{-1} , 465 cm^{-1} , 508 cm^{-1} , 536 cm^{-1} , 567 cm^{-1} , 615 cm^{-1} , 694 cm^{-1} , 770 cm^{-1} , 805 cm^{-1} , and 845 cm^{-1} that can be assigned to barium titanate of stoichiometry $\text{Ba}_2\text{Ti}_9\text{O}_{20}$. Raman spectra shown in Figure 3(a–c) have a very good agreement with work of Javadpour and Eror [25], who detected by Raman spectroscopy $\text{Ba}_2\text{Ti}_9\text{O}_{20}$ phase after long treatment at 1200°C, as well as with work of Xu et al. [26].

The XRD diffraction patterns of the Ba-TN samples after sintering at 900°C–1250°C are shown in Figure 4. The XRD analysis revealed that below 1100°C we observed as a main phase orthorhombic BaTi_4O_9 (JCPDS number 34-0070) and the presence of $\text{BaTi}_5\text{O}_{11}$ (JCPDS number 35-0805) as secondary phase. The increase of the calcination temperature above 1100°C caused the phase transition and crystallization of $\text{Ba}_2\text{Ti}_9\text{O}_{20}$ (JCPDS number 40-0405), but the peaks attributed to BaTi_4O_9 were still visible. These results

TABLE 1: Phase composition [% w/w] of Ba-TN sintered at different temperatures estimated from XRD patterns.

Phase	Temp.				
	900°C	1100°C	1150°C	1200°C	1250°C
BaTi_4O_9	66	42	8	6	6
$\text{BaTi}_5\text{O}_{11}$	34	45	—	—	—
$\text{Ba}_2\text{Ti}_9\text{O}_{20}$	—	13	92	94	94

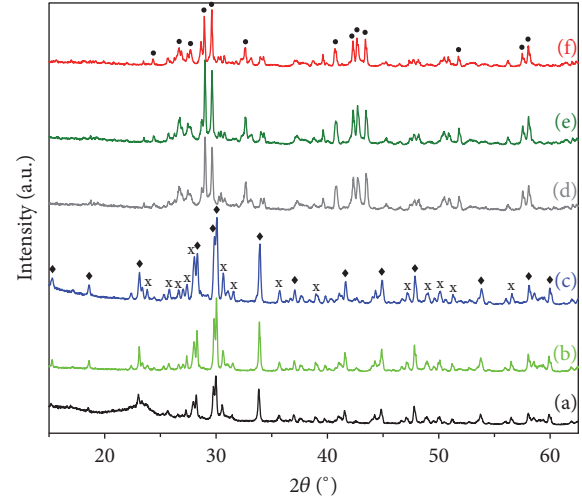


FIGURE 4: XRD patterns of Ba-TN after sintering at (a) 900°C, (b) 950°C, (c) 1100°C, (d) 1150°C, (e) 1200°C, and (f) 1250°C (◆: BaTi_4O_9 ; x: $\text{BaTi}_5\text{O}_{11}$; ●: $\text{Ba}_2\text{Ti}_9\text{O}_{20}$).

are in good agreement with Raman spectra, where phase transformation of BaTi_4O_9 into $\text{Ba}_2\text{Ti}_9\text{O}_{20}$ was also observed for Ba-TN sintered at temperature higher than 1100°C. The quantitative phases composition of the studied samples was estimated on the basis of XRD spectra using the reference intensity ratio (RIR) method [27] and the obtained data are gathered in Table 1. The RIR method involves comparing the intensity of one or more peaks of a phase with the intensity of a peak of a standard (usually the corundum 113 reflection) in a 50 : 50 mixture by weight. For the processing of diffraction data the PANalytical High Score Plus software package was used.

It was found that in the effect of sintering at 900°C the BaTi_4O_9 phase constituted 66% w/w and $\text{BaTi}_5\text{O}_{11}$ 34% w/w of the sample. An increase of the temperature to 1100°C induced certain changes in phase composition. A proportion of BaTi_4O_9 to $\text{BaTi}_5\text{O}_{11}$ phases slightly changed into ratio 42/45% w/w and a new phase showed up – $\text{Ba}_2\text{Ti}_9\text{O}_{20}$ with the content of 11% w/w. The rise of the temperature of only 50°C resulted in very significant changes in phase composition. $\text{BaTi}_5\text{O}_{11}$ phase disappeared completely and new phase, that is, $\text{Ba}_2\text{Ti}_9\text{O}_{20}$ with a content of 92% w/w and BaTi_4O_9 with a content of 8% w/w, was observed. Further increase of sintering temperature up to 1200°C and 1250°C did not influence significantly the phase composition. The $\text{Ba}_2\text{Ti}_9\text{O}_{20}/\text{BaTi}_4\text{O}_9$ weight ratio was estimated at 94/6% w/w for higher sintering temperatures. The observed changes

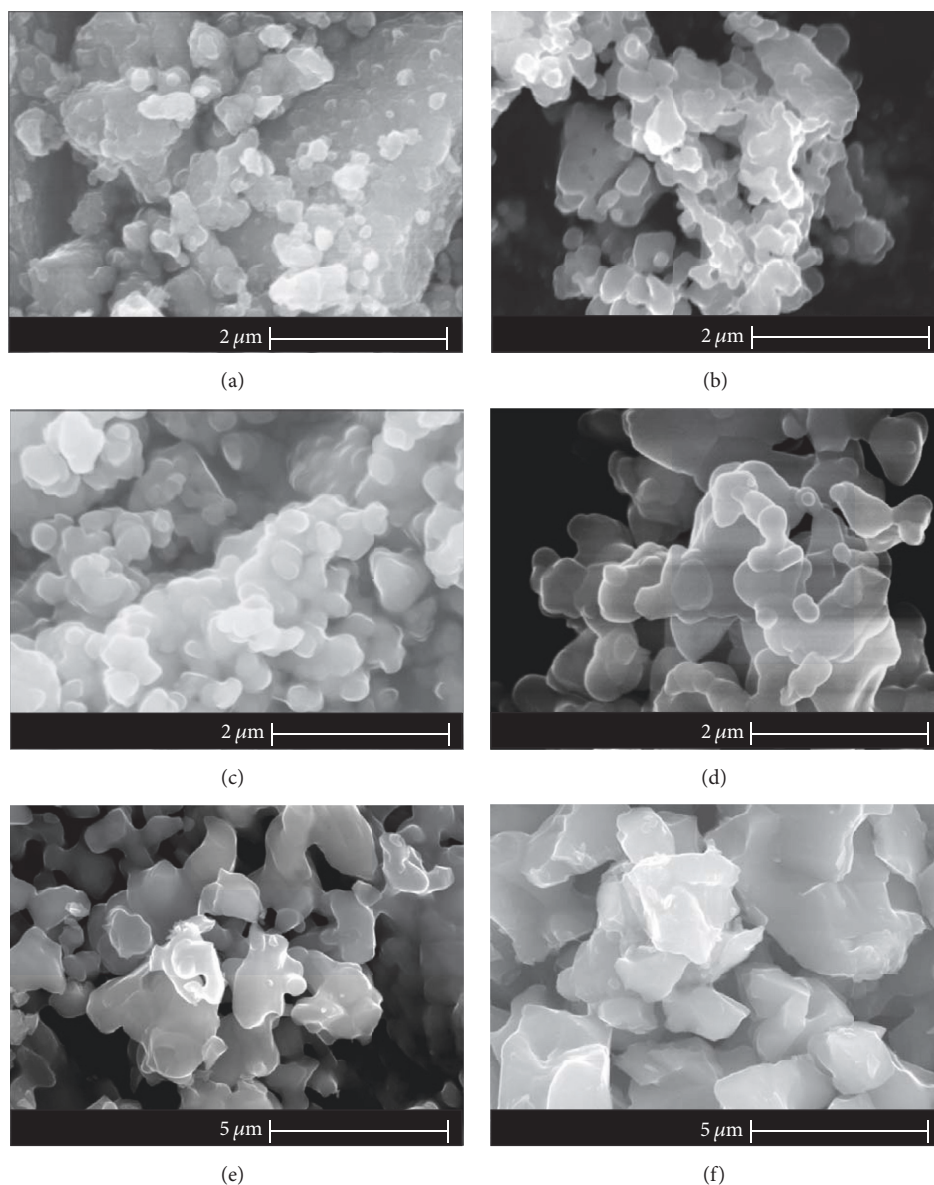


FIGURE 5: SEM images of Ba-TN subjected to step sintering at (a) 500°C, (b) 950°C, (c) 1050°C, (d) 1100°C (magnification 10k), (e) 1150°C, and (f) 1200°C (magnification 25k), collected with accelerating voltage 25 kV.

are in good agreement with observation made by Raman spectroscopy. However, the scattering intensities of $\text{BaTi}_5\text{O}_{11}$ and $\text{Ba}_2\text{Ti}_9\text{O}_{20}$ phases are markedly lower than BaTi_4O_9 . Thus $\text{Ba}_2\text{Ti}_9\text{O}_{20}$ phase was not observed by Raman spectroscopy after the sample sintering at the temperature of 1100°C, but only after treatment at the temperature of 1150°C where the domination of this phase was reached.

Figure 5 illustrates SEM images of Ba-TN powder subjected to calcination at 500°C for 1 hour and sintering for 2 h at the temperature range from 950°C to 1200°C. Mean size of grains and standard deviation, evaluated on the basis of SEM images analysis, are presented in Figure 6, in relation to sintering temperature. The grain size of Ba-TN precursor annealed at 500°C and 950°C kept constant value below 200 nm.

After the sintering at the temperature of 1050°C the particles were still characterized by narrow size distribution and sphere-like grains morphology; however mean size increased to c.a. 400 nm and size distribution significantly widened. A shift of sintering temperature to 1100°C induced evident changes in morphology; partial coarsening of grains occurred. At the temperature of 1150°C and higher, the sphere-like morphology of grains disappeared and irregular agglomerates and large grains were mainly observed. The mean size of grains increases up to about 1.0 μm and 1.6 μm for the temperatures 1150°C and 1200°C, respectively. In the case of Ba-TN sintered at 1200°C irregular agglomerates of rounded shape transformed into sharp angular grains. A marked change in grains' size and morphology observed at the temperature above 1100°C coincides with the structural

TABLE 2: Pellets filling percentage and dielectric properties of the Ba-TN precursor sintered at different temperatures.

Sintering temperature of Ba-TN precursor [°C]	Relative density [%]	Dielectric constant (ϵ) (at 1 MHz)	$\tan(\delta)$ (at 1 MHz)	Quality factor (Q) at 1 MHz	Temperature coefficient (°)ppm/°C
900	64 ^a	25,7	$4,2 * 10^{-4}$	2300	-32
1100	78 ^a	32,4	$8,7 * 10^{-5}$	11500	-18
1200	85 ^b	35,1	$7,7 * 10^{-5}$	13000	7
1250	88 ^b	37,6	$7,5 * 10^{-5}$	13300	33
1300	98 ^b	42,0	$1,5 * 10^{-5}$	66600	37

^aValue calculated in regard to theoretical density of BaTi_4O_9 ; ^bvalue calculated in regard to theoretical density of $\text{Ba}_2\text{Ti}_9\text{O}_{20}$; ^cvalue calculated in a temperature range from -130°C to 100°C .

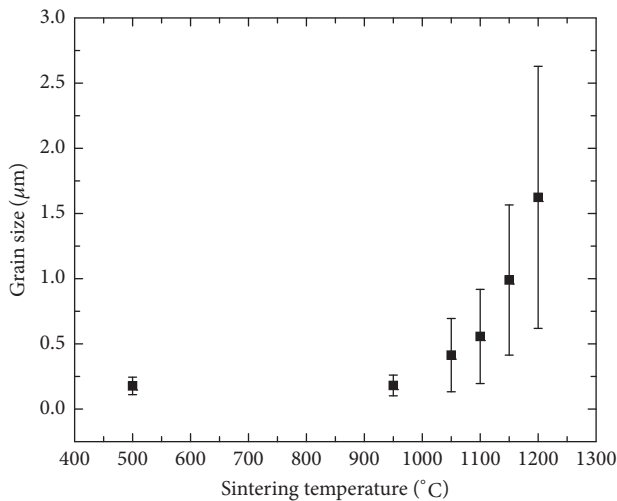


FIGURE 6: Grain size dependence as a function of calcination temperature.

transformation observed by Raman spectroscopy and XRD analysis.

The dielectric parameters of the sintered precursor are strictly dependent on densification behavior, that is, shrinkage of formed discs upon heating. From this reason the relative density and percentage of pellets' filling were investigated as a function of applied step sintering. It is well known that higher temperature of sintering rises these parameters; however in Figures 7(a) and 7(b) one can find some regimes that are distinguished by different behavior below and above temperature of 1050°C . Below this temperature the increase of relative density and percentage of pellets' filling is slow, whereas above 1050°C these parameters rise substantially. This caused a rapid pellet's contraction that can be connected with an acceleration of diffusion in solid state and initiation of neck formation between crystallites above this temperature, that is, in agreement with grains' morphology changes at 1100°C revealed by SEM investigations. Above this temperature there is a phase transformation of main (BaTi_4O_9) and secondary ($\text{BaTi}_5\text{O}_{11}$) phases into $\text{Ba}_2\text{Ti}_9\text{O}_{20}$ and concomitant further increase of pellets' relative density. The percentage of pellets' filling was calculated taking into account the theoretic density values of BaTi_4O_9 and $\text{Ba}_2\text{Ti}_9\text{O}_{20}$ that are equal $4,52\text{ g/cm}^3$ (Pearson's Crystal Data, ICDD 04-007-2688)

and $4,58\text{ g/cm}^3$ (crystallographic data, reference code 00-035-0051), respectively. Finally after sintering at 1250°C calculated relative pellet's density was $4,01\text{ g/cm}^3$ that corresponds to more than 85% of $\text{Ba}_2\text{Ti}_9\text{O}_{20}$ crystallographic density.

To characterize the dielectric properties of sintered at different temperatures Ba-TN pellets we applied broadband dielectric spectroscopy which allowed us to determine the following physical properties that are important for ceramic applications: dielectric permittivity (ϵ), quality factor (Q) defined as $1/\tan(\delta)$, and temperature coefficient of resonant frequency (τ_ϵ). Figure 8 shows three-dimensional graphs comprising the temperature-frequency representations of dielectric permittivity for Ba-TN sintered at 900°C (Figure 8(a)) and 1200°C (Figure 8(b)), respectively. The graphs clearly show that in very broad temperature and frequency ranges there is a lack of any relaxation process in the material. The increase in these variables at low frequencies and at high temperatures is connected with interfacial polarization or electrode polarization contribution that might be present under these conditions. These graphs are exemplary also for Ba-TN precursor sintered in other temperatures.

In Figure 9 the temperature dependence of dielectric permittivity of Ba-TN subjected to sintering at different temperatures is shown. All samples, in MHz frequencies, are characterized by very stable, flat response over broad range of temperatures (more than 230°C). One can observe an increase of ϵ with sintering temperature that is connected to well known relationship between density of the sample and its dielectric properties, according to which higher density results in a higher dielectric permittivity and lower porosity, which improves also quality factor value Q. The relative density of ceramic pellets studied by us was varying from 64 to 96% (Table 2). It means that measured ceramics were partially porous and can be considered as capacitor composed of ceramic and air. Phase composition of measured sample (calculated from XRD, data gathered in Table 1) is another factor influencing dielectric permittivity. In the case of BaTi_4O_9 and $\text{Ba}_2\text{Ti}_9\text{O}_{20}$, the maximum literature values of ϵ were equal to 39 [5] and 52 [28], respectively. The Ba-TN subjected to step sintering in a range of temperatures from 900°C to 1300°C can be considered as a mixture of tetra- and nonatitanates; thus they are expected to possess intermediate dielectric properties. It can be concluded that Ba-TN precursor can be sintered at given temperatures, so that its dielectric permittivity can be tuned between 25 and

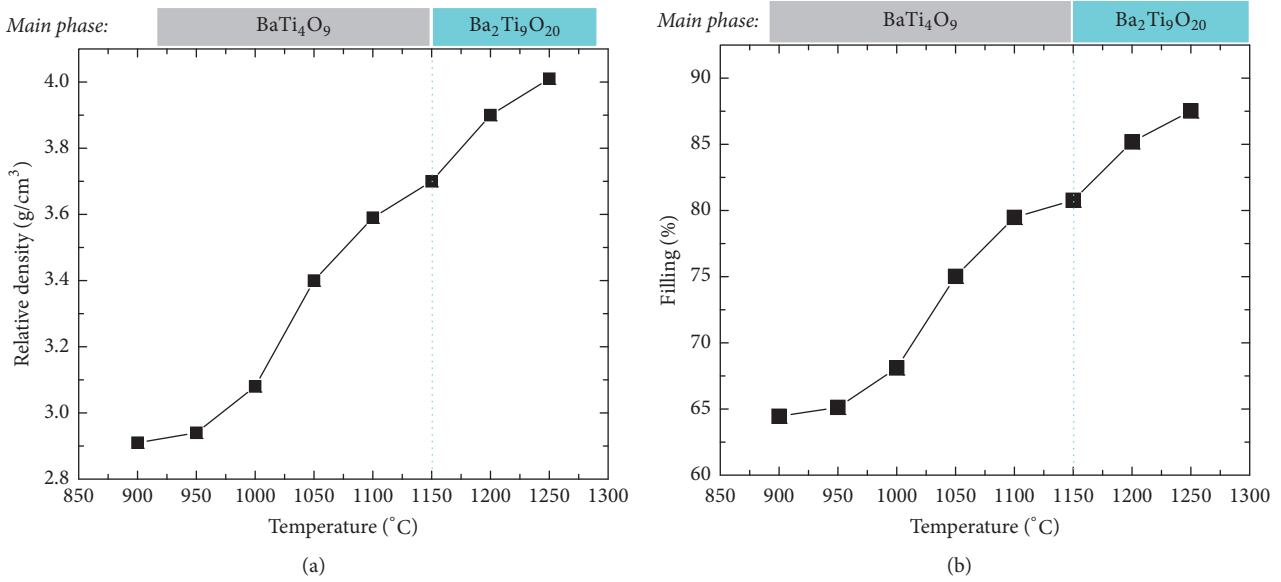


FIGURE 7: Dependence of pellet's relative density (a) and percentage of pellet's filling (b) on the Ba-TN sintering temperature.

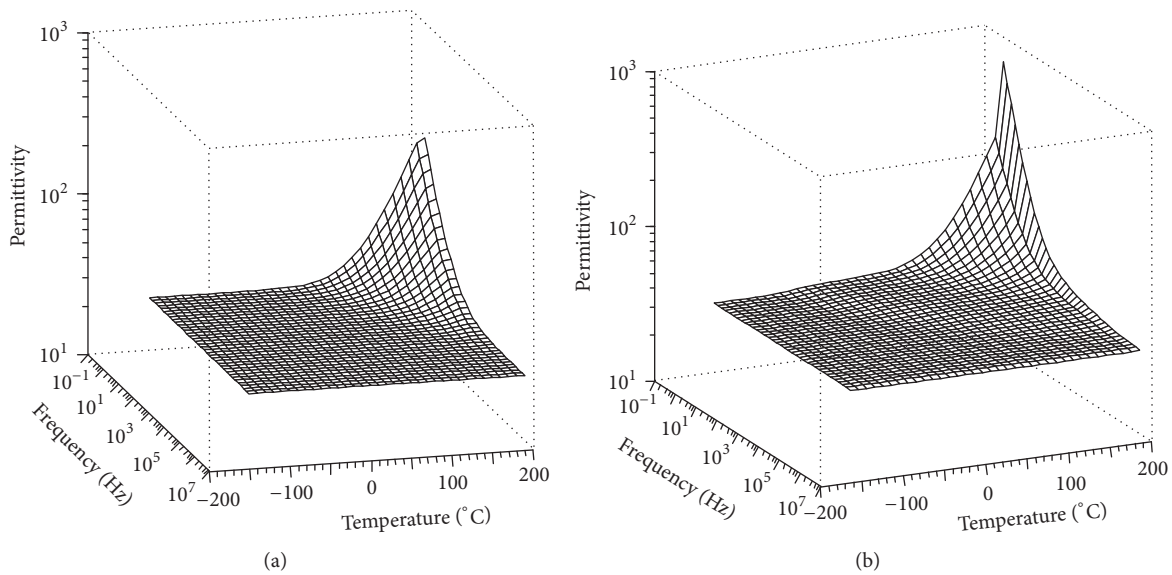


FIGURE 8: Temperature-frequency representation of dielectric permittivity Ba-TN sintered at (a) 900°C and (b) 1200°C.

42. Detected values of $\tan(\delta)$, measured at 20 °C for frequency 1 MHz, were also very interesting and vary from $4,2 \cdot 10^{-4}$ (for Ba-TN sintered at 900 °C) to $1,5 \cdot 10^{-5}$ (for Ba-TN sintered at 1300 °C). The lower value of loss tangent detected for samples sintered at higher temperatures can be connected to higher density of measured pellets. It can be noticed that Q values arise with higher sintering temperature reaching a maximum value of 66,600 for sample sintered at 1300 °C which exhibits the highest density equal to $4,42 \text{ g/cm}^3$, that is, 98% of Ba₂Ti₉O₂₀ theoretical density. This can be associated with a change of porosity, that is, higher density of pellets after treatment at higher temperature and it is in agreement

with a statement according to which the porosity decreases the quality factor due to the presence of moisture in the pores.

From the representations given in Figure 5, the temperature coefficient (τ_ϵ) was calculated as a function of temperature from -130 °C to 100 °C according to (2)

$$\tau_{\epsilon}|_{-130^{\circ}\text{C}}^{100^{\circ}\text{C}} = \frac{1}{\epsilon_{(-130^{\circ}\text{C})}} \left(\frac{\Delta\epsilon}{\Delta T} \right) \text{ ppm}/^{\circ}\text{C}. \quad (2)$$

It was observed that temperature coefficients changed from negative, for Ba-TN sintered up to 1100 °C with BaTi₄O₉ as a main phase, to positive for Ba-TN sintered in a range of

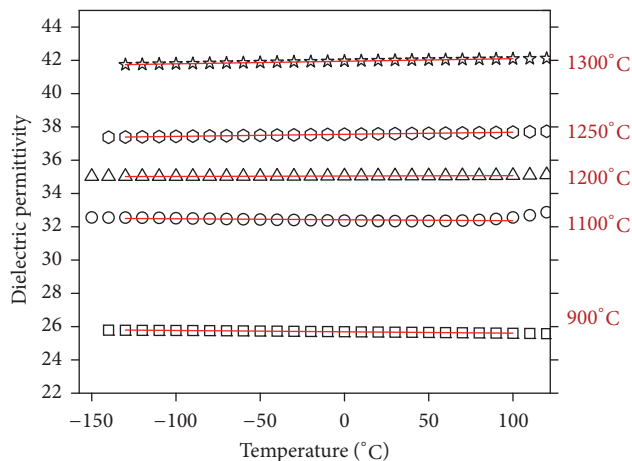


FIGURE 9: The temperature dependence of dielectric permittivity measured at 1.15 MHz of Ba-TN sintered at different temperatures. Red lines correspond to linear fits for calculation of temperature coefficients.

temperatures 1150 ÷ 1300°C with a main phase of $\text{Ba}_2\text{Ti}_9\text{O}_{20}$. This can be connected with phase transformation of BaTi_4O_9 into $\text{Ba}_2\text{Ti}_9\text{O}_{20}$ and low value of temperature coefficient for barium nonatitanate that was found equal to about 6 ppm/°C [28]. It should be emphasized that the dielectric properties of the investigated ceramics depend considerably on sintering temperature and their microstructures. According to this the temperature coefficient for $\text{Ba}_2\text{Ti}_9\text{O}_{20}$ may vary between -6 and 38 ppm/°C [10, 29]. Presented herein are dielectric results which are in agreement with results of Kumar et al. who obtained BaTi_4O_9 and $\text{Ba}_2\text{Ti}_9\text{O}_{20}$ ceramics by the wet chemical gel-carbonate method and found comparable dielectric permittivity, but there was no exact data concerning temperature coefficient values [28].

Obtained within this work are materials which are regarded as three important low loss dielectric ceramics. BaTi_4O_9 and $\text{Ba}_2\text{Ti}_9\text{O}_{20}$ are regarded as stable forms, whereas $\text{BaTi}_5\text{O}_{11}$ is a metastable one. The observed by us transformation is in agreement with phase diagram of BaTiO_3 - TiO_2 system [30], where BaTi_4O_9 is located in the immediate vicinity of $\text{Ba}_2\text{Ti}_9\text{O}_{20}$ and both phases appear to be in equilibrium below 1420°C for compositions between 80 and 81,8 mol% TiO_2 in BaTiO_3 - TiO_2 .

5. Conclusion

Ba-TN precursor obtained from reaction of titanate nanosheets with barium ions was found as an interesting method to obtain barium titanates that exhibit elevated values of dielectric permittivity and low loss tangent in MHz frequencies. The dielectric properties of this composite can be tailored by suitably adjusting the sintering temperatures. According to this barium titanates of stoichiometry, BaTi_4O_9 being the predominant phase and $\text{BaTi}_5\text{O}_{11}$ as minor phase below 1150°C are present, whereas $\text{Ba}_2\text{Ti}_9\text{O}_{20}$ is formed at higher temperatures of sintering. The dielectric properties of these ceramics depend considerably on sintering temperature

and their microstructures. From this reason structural studies as well as grain morphology and dielectric investigations were carried out simultaneously in each step of Ba-TN sintering. It was found that up to temperature of 1050°C barium titanate exhibits fine ceramics grain size. At higher temperature grain morphology radically changes simultaneously with crystallographic phase composition change revealed by XRD and Raman studies.

Conflicts of Interest

The authors declare that they have no conflicts of interest.

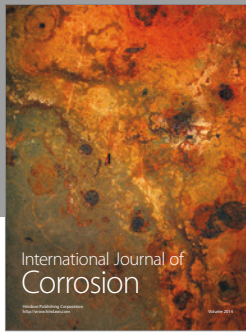
Acknowledgments

This work was financially supported by National Science Center (Poland) grant awarded by Decision no. DEC-2011/03/D/ST5/06074. Izabela Bobowska, Agnieszka Opasinska, and Jacek Ulanski acknowledge financial support by Foundation for Polish Science, Grant Master 9./2013.

References

- [1] M. T. Sebastian, in *Dielectric materials for wireless communication*, Elsevier B.V, Great Britain, 1st edition, 2008.
- [2] D. J. Masse, R. A. Pucel, D. W. Readey, E. A. Maguire, and C. P. Hartwig, "A New Low-Loss High-K Temperature-Compensated Dielectric for Microwave Applications," *Proceedings of the IEEE*, vol. 59, no. 11, pp. 1628-1629, 1971.
- [3] S. G. Mhaisalkar, W. E. Lee, and D. W. Readey, "Processing and Characterization of BaTi_4O_9 ," *Journal of the American Ceramic Society*, vol. 72, no. 11, pp. 2154-2158, 1989.
- [4] S. G. Mhaisalkar, D. W. Readey, and S. A. Akbar, "Microwave Dielectric Properties of Doped BaTi_4O_9 ," *Journal of the American Ceramic Society*, vol. 74, no. 8, pp. 1894-1898, 1991.
- [5] M. Cernea, E. Chirtop, D. Neacsu, I. Pasuk, and S. Iordanescu, "Preparation of BaTi_4O_9 from oxalates," *Journal of the American Ceramic Society*, vol. 85, no. 2, pp. 499-503, 2002.
- [6] J. Choy, Y. Han, J. Sohn, and M. Itoh, "Microwave Characteristics of BaO-TiO_2 Ceramics Prepared via a Citrate Route," *Journal of the American Ceramic Society*, vol. 78, no. 5, pp. 1169-1172, 1995.
- [7] F. Li, L.-Q. Weng, G.-Y. Xu, S.-H. Song, and J. Yu, "Synthesis and characterization of microwave dielectric BaTi_4O_9 ceramics via EDTA-citrate gel process," *Materials Letters*, vol. 59, no. 23, pp. 2973-2976, 2005.
- [8] K. Fukuda, R. Kitoh, and I. Awai, "Microwave characteristics of mixed phases of BaTi_4O_9 - $\text{BaPr}_2\text{Ti}_4\text{O}_{12}$ ceramics," *Journal of Materials Science*, vol. 30, no. 5, pp. 1209-1216, 1995.
- [9] E. Tillmanns, "Die Kristallstruktur von $\text{BaTi}_5\text{O}_{11}$," *Acta Crystallographica Section B*, vol. 25, p. 1444, 1969.
- [10] J.-H. Choy, Y.-S. Han, J.-T. Kim, and Y.-H. Kim, "Citrate route to ultra-fine barium polytitanates with microwave dielectric properties," *Journal of Materials Chemistry*, vol. 5, no. 1, pp. 57-63, 1995.
- [11] H. Lu, L. E. Burkhart, and G. L. Schrader, "Sol-Gel Process for the Preparation of $\text{Ba}_2\text{Ti}_9\text{O}_{20}$ and $\text{BaTi}_5\text{O}_{11}$," *Journal of the American Ceramic Society*, vol. 74, no. 5, pp. 968-972, 1991.

- [12] T. Fukui, C. Sakurai, and M. Okuyama, "Effects of heating rate on sintering of alkoxide-derived BaTi₅O₁₁ powder," *Journal of Materials Research*, vol. 7, no. 1, pp. 192–196, 1992.
- [13] S.-F. Wang, Y.-F. Hsu, T.-H. Ueng, C.-C. Chiang, J. P. Chu, and C.-Y. Huang, "Effects of additives on the microstructure and dielectric properties of Ba₂Ti₉O₂₀ microwave ceramic," *Journal of Materials Research*, vol. 18, no. 5, pp. 1179–1187, 2003.
- [14] T.-T. Fang, J.-T. Shiue, and S.-C. Liou, "Formation mechanism and sintering behavior of Ba₂Ti₉O₂₀," *Journal of the European Ceramic Society*, vol. 22, no. 1, pp. 79–85, 2002.
- [15] K. P. Surendran, P. Mohanan, and M. T. Sebastian, "Tailoring the microwave dielectric properties of GdTiNb_{1-x}TaxO₆ and Sm_{1-x}Y_xTiTaO₆ ceramics," *Journal of the European Ceramic Society*, vol. 23, no. 14, pp. 2489–2495, 2003.
- [16] T. Sasaki, F. Kooli, M. Iida et al., "A mixed alkali metal titanate with the lepidocrocite-like layered structure. Preparation, crystal structure, protonic form, and acid-base intercalation properties," *Chemistry of Materials*, vol. 10, no. 12, pp. 4123–4128, 1998.
- [17] W. A. England, J. E. Birkett, J. B. Goodenough, and P. J. Wiseman, "Ion exchange in the Cs_x[Ti_{2-x/2}Mgx/2]O₄ structure," *Journal of Solid State Chemistry*, vol. 49, no. 3, pp. 300–308, 1983.
- [18] E. Chiellini, J. Sunamoto, C. Migliaresi, R. M. Ottenbrite, and D. Cohn, *Biomedical Polymers and Polymer Therapeutics*, Kluwer Academic Publishers, Boston, 2002.
- [19] I. Bobowska, A. Opasińska, A. Wypych, and P. Wojciechowski, "Synthesis and dielectric investigations of ZnTiO₃ obtained by a soft chemistry route," *Materials Chemistry and Physics*, vol. 134, no. 1, pp. 87–92, 2012.
- [20] G. Pfaff, "Synthesis and characterization of BaTi₄O₉," *Journal of Materials Science Letters*, vol. 10, no. 3, pp. 129–131, 1991.
- [21] T. Ohya, A. Nakayama, T. Ban, Y. Ohya, and Y. Takahashi, "Synthesis and characterization of halogen-free, transparent, aqueous colloidal titanate solutions from titanium alkoxide," *Chemistry of Materials*, vol. 14, no. 7, pp. 3082–3089, 2002.
- [22] T. Gao, H. Fjellvag, and P. Norby, *Journal of Physical Chemistry B*, vol. 112, p. 9400, 2008.
- [23] N. Li, L. Zhang, Y. Chen, M. Fang, J. Zhang, and H. Wang, "Highly efficient, irreversible and selective ion exchange property of layered titanate nanostructures," *Advanced Functional Materials*, vol. 22, no. 4, pp. 835–841, 2012.
- [24] M. Rössel, H.-R. Höche, H. S. Leipner et al., "Raman microscopic investigations of BaTiO₃ precursors with core-shell structure," *Analytical and Bioanalytical Chemistry*, vol. 380, no. 1, pp. 157–162, 2004.
- [25] J. Javadpour and N. G. Eror, "Raman Spectroscopy of Higher Titanate Phases in the BaTiO₃-TiO₂ System," *Journal of the American Ceramic Society*, vol. 71, no. 4, pp. 206–213, 1988.
- [26] Y. Xu, X. Yuan, G. Huang, and H. Long, "Polymeric precursor synthesis of Ba₂Ti₉O₂₀," *Materials Chemistry and Physics*, vol. 90, no. 2-3, pp. 333–338, 2005.
- [27] F. H. Chung, *Journal of Applied Crystallography*, vol. 7, p. 519, 1974.
- [28] S. Kumar, V. S. Raju, and T. R. N. Kutty, "Preparation of BaTi₄O₉ and Ba₂Ti₉O₂₀ ceramics by the wet chemical gel-carbonate method and their dielectric properties," *Materials Science and Engineering B: Solid-State Materials for Advanced Technology*, vol. 142, no. 2-3, pp. 78–85, 2007.
- [29] C.-L. Huang, M.-H. Weng, C.-T. Lion, and C.-C. Wu, "Low temperature sintering and microwave dielectric properties of Ba₂Ti₉O₂₀ ceramics using glass additions," *Materials Research Bulletin*, vol. 35, no. 14-15, pp. 2445–2456, 2000.
- [30] K. W. Kirby and B. A. Wechsler, "Phase relations in the Barium Titanate—Titanium Oxide System," *Journal of the American Ceramic Society*, vol. 74, no. 8, pp. 1841–1847, 1991.



Hindawi

Submit your manuscripts at
<https://www.hindawi.com>

